



Local environment of silicon in cubic boron nitride

Hidenobu Murata, Takashi Taniguchi, Shunichi Hishita, Tomoyuki Yamamoto, Fumiyasu Oba, and Isao Tanaka

Citation: *Journal of Applied Physics* **114**, 233502 (2013); doi: 10.1063/1.4849015

View online: <http://dx.doi.org/10.1063/1.4849015>

View Table of Contents: <http://scitation.aip.org/content/aip/journal/jap/114/23?ver=pdfcov>

Published by the [AIP Publishing](#)



Re-register for Table of Content Alerts

Create a profile.



Sign up today!



Local environment of silicon in cubic boron nitride

Hideobu Murata,^{1,a)} Takashi Taniguchi,¹ Shunichi Hishita,² Tomoyuki Yamamoto,³ Fumiyasu Oba,⁴ and Isao Tanaka^{4,5}

¹Advanced Key Technologies Division, National Institute for Materials Science, 1-1 Namiki Tsukuba, Ibaraki 305-0044, Japan

²Environment and Energy Materials Division, National Institute for Materials Science, 1-1 Namiki Tsukuba, Ibaraki 305-0044, Japan

³Faculty of Science and Engineering, Waseda University, 3-4-1 Okubo, Shinjuku, Tokyo 169-8555, Japan

⁴Department of Materials Science and Engineering, Kyoto University, Yoshida-Honmachi, Sakyo, Kyoto 606-8501, Japan

⁵Nanostructures Research Laboratory, Japan Fine Ceramics Center, 2-4-1 Mutsuno, Atsuta, Nagoya 456-8587, Japan

(Received 12 November 2013; accepted 2 December 2013; published online 16 December 2013)

Si-doped cubic boron nitride (*c*-BN) is synthesized at high pressure and high temperature, and the local environment of Si is investigated using X-ray absorption near edge structure (XANES) and first-principles calculations. Si-*K* XANES indicates that Si in *c*-BN is surrounded by four nitrogen atoms. According to first-principles calculations, the model for substitutional Si at the B site well reproduces experimental Si-*K* XANES, and it is energetically more favorable than substitutional Si at the N site. Both the present experimental and theoretical results indicate that Si in *c*-BN prefers the B site to the N site. © 2013 AIP Publishing LLC. [<http://dx.doi.org/10.1063/1.4849015>]

I. INTRODUCTION

Cubic boron nitride (*c*-BN) is a high-density phase of BN and has a similar crystal structure and properties to diamond. Its applications widely vary from a super-hard material to opt-electronics. Bulk *c*-BN was first synthesized under high-pressure, high-temperature (HPHT) conditions by Wentorf.¹ During syntheses, defects and coexistent elements are often incorporated into *c*-BN and behave as the origin of various properties. It has been reported that *c*-BN shows both *n*- and *p*-type conductivity,^{2,3} ultraviolet light emission from its *p*-*n* junction,⁴ and luminescence,⁵⁻⁸ for example.

The electronic and atomistic structures of dopants and defects in *c*-BN have attracted much research attention. Although there have been a number of theoretical studies reporting on native defects⁹⁻¹⁴ and dopants,^{11,15-23} it is difficult to experimentally reveal the atomistic structure of trace dopants. Recently, a combined scanning transmission electron microscopy (STEM) and first-principles study found that luminous Ce³⁺ is incorporated into *c*-BN by the following unusual mechanism: Ce³⁺ in *c*-BN is not substituted for the cationic B site but for the anionic N site with surrounding B-vacancies.²³ Therefore, it is necessary to revisit the local environments of dopants in *c*-BN.

X-ray absorption near edge structure (XANES) is a powerful tool to investigate dopants. It reveals local electronic and atomistic structures with elemental selectivity. A number of dopants in various types of material have been investigated using XANES.²⁴ Since XANES analyses are based on the “finger printing” method, theoretical calculations are helpful to interpret the spectra of dopants. This

method enables us to determine the local environment of trace dopants.^{25,26}

Si is one of the *n*-type dopants that are found at the initial stage of the development of *c*-BN.² In this study, we synthesized Si-doped *c*-BN under HPHT conditions and investigated the local environment of Si using XANES and first-principles calculations.

II. EXPERIMENTAL AND COMPUTATIONAL PROCEDURES

A. Sample preparation

Si-doped *c*-BN samples were synthesized with a Si solvent under HPHT conditions.²⁷ Si wafers (99.999%, Rare-metallic Co., Ltd.), commercial *h*-BN sintered disks (type N-1, Denka Co., Ltd.), and *h*-BN powder (type GP, Denka Co., Ltd.) were used as the starting materials. Before syntheses, deoxygenation of *h*-BN was carried out at 1500 °C in N₂ flow and at 1950 °C in vacuum. Sample assembly for HPHT treatments was similar to that of Ref. 27; we used a Si wafer and an MgO capsule instead of Si powder and a Ta capsule. HPHT treatments were performed with a belt-type high-pressure apparatus FB-30H. Pressure and temperature were determined in the same manner as that described in Ref. 28. Samples were kept at 7.7 GPa and 1700 °C for 1 h and then quenched to room temperature. MgO capsules were removed by nitro hydrochloric acid. The samples were then soaked in a mixture of HNO₃ and HF at 150 °C for 12 h in order to remove residual Si and *h*-BN.

B. Characterization

The samples were characterized using X-ray diffraction (XRD), secondary ion mass spectrometry (SIMS), and XANES. XRD patterns were collected by Rigaku RINT2200V/PC with a Cu-*K*α target and a graphite counter monochromator. For SIMS measurements, the Si-doped

^{a)}Research Fellow of Japan Society for the Promotion of Science. Author to whom correspondence should be addressed. Electronic mail: MURATA.Hideobu@nims.go.jp

c-BN samples were sintered at 7.7 GPa and 2150 °C. Details of the sintering method have been reported elsewhere.²⁹ The SIMS measurements were conducted with PHI ADEPT1010 using a Cs⁺ beam. The primary beam acceleration voltage was 5.0 kV. Undoped *c*-BN polycrystals for the SIMS standard specimen were prepared by high-pressure reaction sintering from *h*-BN at 7.7 GPa and 2200 °C without additives. Si-ion implantation was applied to the polished specimen at an energy of 65 keV, a dose of 1×10^{15} ion/cm², and an ion current of 36 nA/cm². Si-K XANES was measured by the total electron yield method with an InSb double-crystal monochromator at BL2A in UVSOR, Okazaki, Japan.

C. First-principles calculations

1. Formation enthalpy

The formation enthalpies and atomistic structures of Si dopants in *c*-BN at 0 and 7.7 GPa were calculated with the plane-wave basis projector augmented wave method³⁰ implemented in the Vienna *Ab-initio* Simulation Package (VASP) code.^{31,32} The cut-off energy of plane waves was set to 600 eV. The exchange-correlation functional was given by the generalized gradient approximation presented by Perdew, Burke, and Ernzerhof (GGA-PBE).³³ Si-doped *c*-BN was modeled using a $4 \times 4 \times 4$ 128-atom supercell of *c*-BN. The *k*-point sampling was carried out with Monkhorst-Pack $2 \times 2 \times 2$ mesh.³⁴ Structural parameters were fully optimized until the residual forces were less than 0.02 eV/Å and the deviations in stress from the target values, i.e., 0 and 7.7 GPa, were less than 0.05 GPa. The calculated lattice constant at 0 GPa is 3.625 Å, which is close to an experimental value of 3.6159(1) Å.³⁵ Convergence tests with a cut-off energy of 800 eV and $4 \times 4 \times 4$ *k*-mesh indicated that the total energies converged within less than 3 meV/atom.

In the *c*-BN crystal, Si might be substituted for both B and N sites. In order to discuss the stability of these configurations, defect formation enthalpies were estimated.³⁶ The formation enthalpy of a defect in charge state *q* is given as

$$\Delta H = H_{\text{def}} - \sum_i n_i \mu_i + q \varepsilon_F,$$

where H_{def} , n_i , μ_i , and ε_F are the enthalpy of a defective supercell, the number of atoms and the atomic chemical potential for element *i*, and the Fermi level, respectively. The atomic chemical potentials were determined by equilibrium conditions based on the experimental observation that *c*-BN was formed at the boundary between *h*-BN and Si. In order to simulate this experimental situation, we assumed two equilibrium conditions, BN-Si-B and BN-Si-Si₃N₄, denoted as B- and N-rich conditions, respectively. We adopted *c*-BN, diamond-type Si, and β -B and β -Si₃N₄ phases, and their enthalpies were used as the chemical potentials of these host and reference phases, $\mu_{\text{BN}(\text{bulk})}$, $\mu_{\text{Si}(\text{bulk})}$, $\mu_{\text{B}(\text{bulk})}$, and $\mu_{\text{Si}_3\text{N}_4(\text{bulk})}$. The chemical potential of Si was given as $\mu_{\text{Si}} = \mu_{\text{Si}(\text{bulk})}$ under both B- and N-rich conditions, and those of B and N were determined by $\mu_{\text{B}} = \mu_{\text{B}(\text{bulk})}$ and $\mu_{\text{B}} + \mu_{\text{N}} = \mu_{\text{BN}(\text{bulk})}$ under the B-rich condition, and $3\mu_{\text{Si}} + 4\mu_{\text{N}} = \mu_{\text{Si}_3\text{N}_4(\text{bulk})}$ and $\mu_{\text{B}} + \mu_{\text{N}} = \mu_{\text{BN}(\text{bulk})}$ under the N-rich condition. The Fermi level in the Si-doped *c*-BN sample is unknown, and therefore, it was treated as a variable

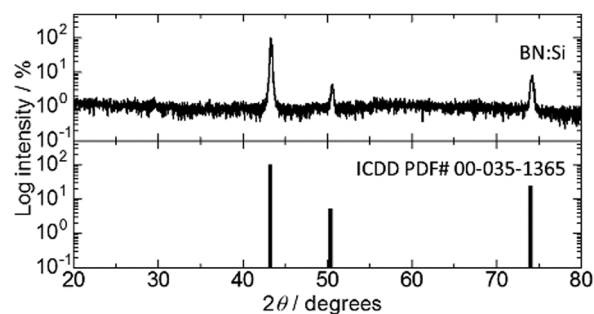


FIG. 1. XRD pattern of a Si-doped *c*-BN sample after acid treatments.

between the valence band maximum (VBM) and conduction band minimum (CBM). In order to correct the finite-size effects of the supercells with charged defects, we employed approximate third-order image charge corrections reported in Ref. 37 in conjunction with electrostatic potential alignment suggested in Ref. 38.

2. XANES simulations

Theoretical Si-K XANES spectra were calculated using the augmented plane-wave + local orbitals (APW + *lo*) method implemented in the WIEN2k code.³⁹ $R_{\text{MT}}K_{\text{MAX}}$ was set to 6.0 bohrs Ry^{1/2}. R_{MTs} were set to 1.30, 1.30, and 1.50 bohrs for B, N, and Si, respectively. A core-hole effect was included in the final (excited) state calculations. The same models and *k*-mesh as those in the formation enthalpy calculations were employed. Calculated spectra were broadened by Lorentz functions with a natural width of Si-K shell.⁴⁰ Convergence tests on $R_{\text{MT}}K_{\text{MAX}}$ and *k*-mesh confirmed that the transition energy of Si-K XANES was converged within 0.01 eV. The transition energy of Si-K XANES was corrected via the alignment of the strongest peak of α -Si₃N₄ between the theoretical and experimental spectra. In other words, all the calculated spectra were rigidly shifted by −9.1 eV.

III. RESULTS AND DISCUSSIONS

After the HPHT treatment, the samples were recovered as aggregate form. Figure 1 shows the powder XRD pattern

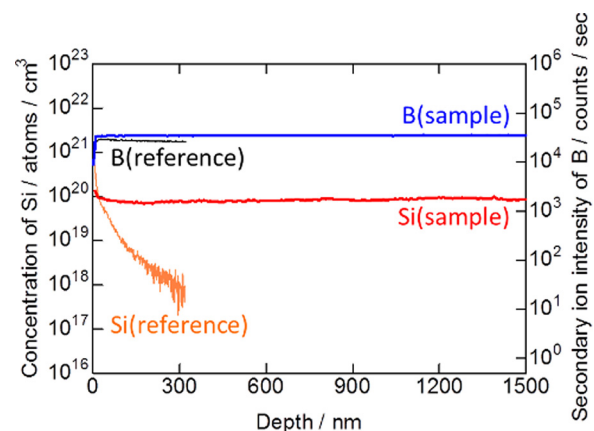


FIG. 2. SIMS depth profiles of a Si-doped *c*-BN sample and references. Red and blue thick lines show the concentration of Si and the secondary ion intensity of B for the *c*-BN sample. Orange and black thin lines denote those of the references.

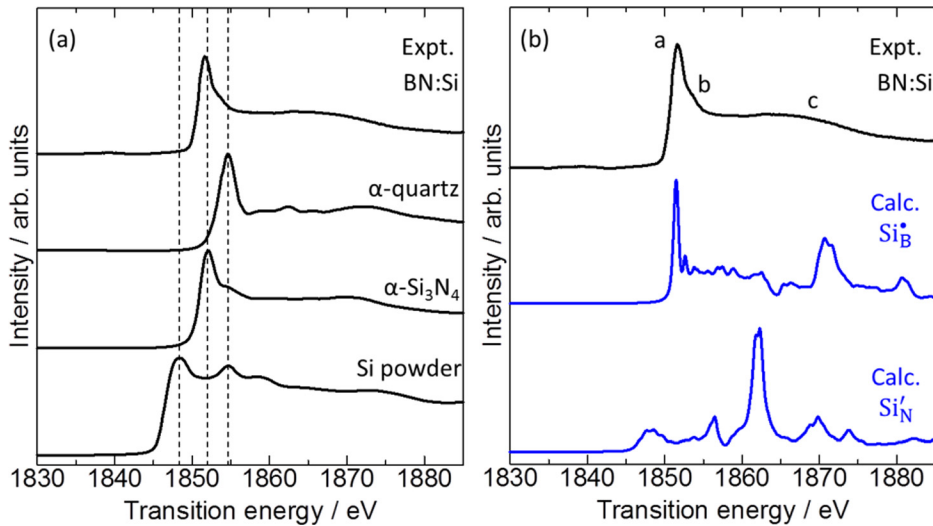


FIG. 3. (a) Experimental Si-K XANES of Si-doped *c*-BN and references. Note that the Si powder is partially oxidized and a SiO₂ peak is detected at 1855 eV in its spectrum. The vertical dashed lines indicate the main peak in the reference spectra. (b) Experimental (black) and calculated (blue) Si-K XANES of Si-doped *c*-BN. The calculated spectra are rigidly shifted by -9.1 eV (see text) and broadened by Lorenz functions with a natural width.⁴⁰

of a Si-doped *c*-BN sample after the acid treatment. All of the peaks can be assigned to *c*-BN (ICDD PDF 35-1355). Si-doped *c*-BN powder was treated at 7.7 GPa and 2150 °C so as to sinter as a disk shape without any additives. The concentration of Si in the sintered body was characterized using SIMS. As shown in Figure 2, there are 10^{20} atoms/cm³ of Si. The concentration of Si does not depend on the depth from the surfaces to the inner parts, suggesting a homogeneous distribution of Si in the *c*-BN bodies.

In order to analyze the local environment of Si in *c*-BN samples, Si-K XANES was measured. Figure 3(a) shows the Si-K XANES of Si-doped *c*-BN and reference materials. Si-K XANES clearly exhibits chemical shifts. Note that Si₃N₄ has a lower transition energy than SiO₂ although the formal charge of Si is the same. The spectrum of Si-doped *c*-BN has a similar feature to α -Si₃N₄, but the fine structure is different in that the shoulder peak of Si-doped *c*-BN lies at a lower energy than that of α -Si₃N₄ at 1855 eV, for example. The chemical shift of Si-doped *c*-BN is almost the same as α -Si₃N₄. These results imply that there are Si-N bonds and Si⁴⁺ in *c*-BN.

For a detailed analysis of the experimental spectra, Si-K XANES were simulated by first-principles calculations. In our models, Si was substituted for the B or N sites. Since the experimental Si-K XANES indicates that Si in our samples has a similar chemical shift to α -Si₃N₄ with tetravalent Si, we adopted charged defect models, Si_B[•] (singly positively charged) and Si_N[•] (singly negatively charged), which were represented in Kröger-Vink notation. Figure 3(b) shows the

calculated Si-K XANES of Si-substituted *c*-BN. These models present clearly different features. Si_B[•] has similar features to the experimental spectrum: the strongest peak A, shoulder B, and weak peak C in the calculated spectrum. In addition, this model reproduces the chemical shift. In contrast, Si_N[•] has an absorption edge around 1845 eV and the strongest peak at 1863 eV. These features are different from those of the experimental spectrum.

Figure 4 shows the calculated formation enthalpies of Si-doped *c*-BN at 7.7 GPa as a function of the Fermi level. Under both of the B- and N-rich conditions and any Fermi level position, the models for substitutional Si at the B site are more stable than those for the N site. Lowther also reported that Si_B[•] is more stable than Si_N[•] based on the results of first-principles calculations using the local density approximation.²⁰ In our results, there are two stable models, Si_B[•] (singly positively charged) and Si_B[×] (neutral), depending on the Fermi level. It is worth mentioning that the calculated Si-K XANES spectra of these models have qualitatively the same shapes. The Fermi level that changes the charge state corresponds to the ionization energy when measured from the VBM or CBM. The ionization energy from Si_B[×] to Si_B[•] is 0.18 eV at 7.7 GPa and 0.15 eV at 0 GPa, which underestimates the experimental value at ambient pressure, 0.24 eV.⁴¹ For more precise discussions, however, we need a larger cell and a more accurate but computationally demanding approximation such as *GW* or a hybrid functional, which is beyond the scope of this study. In fact, our previous work using a 432-atom cell and the PBE0 hybrid functional yielded an

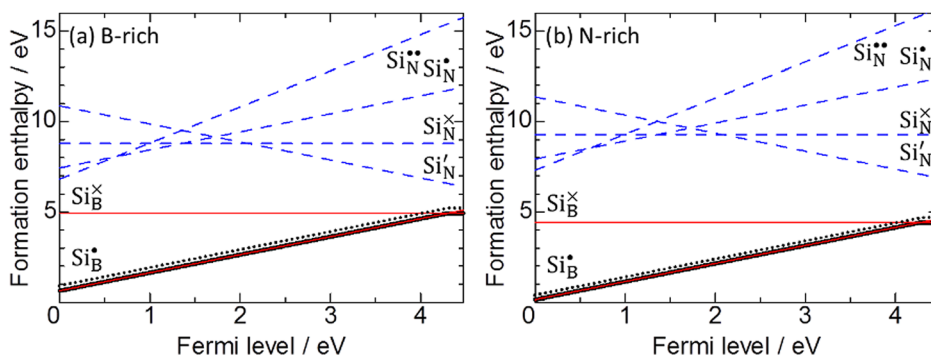


FIG. 4. Formation enthalpies of substitutional Si in *c*-BN as a function of the Fermi level under (a) B-rich and (b) N-rich conditions. Solid red, dashed blue, and bold black lines indicate the values for the B and N sites and the minimum at 7.7 GPa, respectively. The minimum at 0 GPa is also indicated by the dotted black line. Note that the calculated band gap only slightly depends on pressure: 4.45 and 4.47 eV at 0 and 7.7 GPa, respectively.

ionization energy of 0.18 eV at 0 GPa.²² The formation enthalpy of Si_B has a tendency to slightly decrease at high pressure. This stabilization mainly results from a relatively large increase in $\mu_{\text{Si}}(\text{bulk})$ given by diamond-type Si due to its largest volume and hence PV term in enthalpy among the substances considered in this study.

IV. CONCLUSION

Si-doped *c*-BN was synthesized under HPHT conditions, and the local environment of Si was investigated. The XRD pattern can be assigned to *c*-BN without any secondary phases. According to the SIMS measurements, there were 10^{20} atoms/cm³ of Si in the *c*-BN sample. The Si-*K* XANES of the Si-doped *c*-BN sample has a similar feature to α -Si₃N₄, which implies that Si is bonded to N. According to the first-principles calculations, the model for substitutional Si at the B site, Si_B^{*}, reasonably reproduces the experimental Si-*K* XANES spectrum. From an energetic point of view, the model for substitutional Si at the B site is more favorable than that for the N site. The experimental and theoretical results consistently indicate that Si in *c*-BN is substituted for B.

ACKNOWLEDGMENTS

This work was supported by JSPS KAKENHI Grant No. 24-10639 (Grant-in-Aid for JSPS Fellows), the Use-of-UVSOR Facility Program (BL2A, No. 24-502) of the Institute for Molecular Science, and MEXT Elements Strategy Initiative to Form Core Research Center.

- ¹R. H. Wentorf, Jr., *J. Chem. Phys.* **34**, 809–812 (1961).
- ²R. H. Wentorf, Jr., *J. Chem. Phys.* **36**, 1990–1991 (1962).
- ³T. Taniguchi, T. Teraji, S. Koizumi, K. Watanabe, and S. Yamaoka, *Jpn. J. Appl. Phys., Part 2* **41**, L109–L111 (2002).
- ⁴O. Mishima, J. Tanaka, S. Yamaoka, and O. Fukunaga, *Science* **238**, 181–183 (1987).
- ⁵E. M. Shishonok, A. R. Philipp, N. A. Shishonok, and N. G. Anichenko, *Phys. Status Solidi B* **242**, 1700–1704 (2005).
- ⁶A. Nakayama, T. Taniguchi, Y. Kubota, K. Watanabe, and S. Hishita, *Appl. Phys. Lett.* **87**, 211913 (2005).
- ⁷E. M. Shishonok, S. V. Leonchik, J. W. Steeds, and D. Wolverson, *Diamond Relat. Mater.* **16**, 1602–1607 (2007).
- ⁸E. M. Shishonok, L. Trinkler, S. V. Leonchik, and B. Berzinya, *J. Appl. Spectrosc.* **75**, 567–575 (2008).
- ⁹V. A. Gubanov, Z. W. Lu, B. M. Klein, and C. Y. Fong, *Phys. Rev. B* **53**, 4377 (1996).
- ¹⁰P. Piquini, R. Mota, T. M. Schmidt, and A. Fazzio, *Phys. Rev. B* **56**, 3556 (1997).
- ¹¹J. L. P. Castineira, J. R. Leite, L. M. R. Scolfaro, R. Enderlein, J. L. A. Alves, and H. W. Leite Alves, *Mater. Sci. Eng., B* **51**, 53–57 (1998).
- ¹²W. Orellana and H. Chacham, *Appl. Phys. Lett.* **74**, 2984 (1999).
- ¹³W. Orellana and H. Chacham, *Phys. Rev. B* **63**, 125205 (2001).
- ¹⁴F. Tian, Z. Liu, Y. Ma, T. Cui, B. Liu, and G. Zou, *Solid State Commun.* **143**, 532–536 (2007).
- ¹⁵I. A. Howard, *Solid State Commun.* **99**, 697–700 (1996).
- ¹⁶V. A. Gubanov, E. A. Pentaleri, C. Y. Fong, and B. M. Klein, *Phys. Rev. B* **56**, 13077 (1997).
- ¹⁷J. L. P. Castineira, J. R. Leite, J. L. F. da Silva, L. M. R. Scolfaro, J. L. A. Alves, and H. W. L. Alves, *Phys. Status Solidi B* **210**, 401 (1998).
- ¹⁸L. E. Ramos, J. Furthmüller, L. M. R. Scolfaro, J. R. Leite, and F. Bechstedt, *Phys. Rev. B* **66**, 075209 (2002).
- ¹⁹B. Szűcs, A. Gali, Z. Hajnal, P. Deák, and C. G. Van de Walle, *Phys. Rev. B* **68**, 085202 (2003).
- ²⁰J. E. Lowther and I. J. Sigalas, *Diamond Relat. Mater.* **15**, 67–70 (2006).
- ²¹F. Tian, Y. Liu, Y. Ma, T. Cui, B. Liu, and G. Zou, *Diamond Relat. Mater.* **17**, 2025–2028 (2008).
- ²²F. Oba, A. Togo, I. Tanaka, K. Watanabe, and T. Taniguchi, *Phys. Rev. B* **81**, 075125 (2010).
- ²³R. Ishikawa, N. Shibata, F. Oba, T. Taniguchi, S. D. Findlay, I. Tanaka, and Y. Ikuhara, *Phys. Rev. Lett.* **110**, 065504 (2013).
- ²⁴I. Tanaka, T. Mizoguchi, and T. Yamamoto, *J. Am. Ceram. Soc.* **88**, 2013–2029 (2005).
- ²⁵I. Tanaka, T. Mizoguchi, M. Matsui, S. Yoshioka, H. Adachi, T. Yamamoto, T. Okajima, M. Umesaki, W. Y. Ching, Y. Inoue, M. Mizuno, H. Araki, and Y. Shirai, *Nature Mater.* **2**, 541–545 (2003).
- ²⁶M. Ohkubo, S. Shiki, M. Ukibe, N. Matsubayashi, Y. Kitajima, and S. Nagamachi, *Sci. Rep.* **2**, 831 (2012).
- ²⁷D. W. He, M. Akaishi, and T. Tanaka, *Diamond Relat. Mater.* **10**, 1465–1469 (2001).
- ²⁸T. Taniguchi and S. Yamaoka, *J. Cryst. Growth* **222**, 549–557 (2001).
- ²⁹T. Taniguchi, M. Akaishi, and S. Yamaoka, *J. Mater. Res.* **14**, 162–169 (1999).
- ³⁰P. E. Blöchl, *Phys. Rev. B* **50**, 17953 (1994).
- ³¹G. Kresse and J. Furthmüller, *Phys. Rev. B* **54**, 11169 (1996).
- ³²G. Kresse and D. Joubert, *Phys. Rev. B* **59**, 1758 (1999).
- ³³J. P. Perdew, K. Burke, and M. Ernzerhof, *Phys. Rev. Lett.* **77**, 3865 (1996).
- ³⁴H. J. Monkhorst and J. D. Pack, *Phys. Rev. B* **13**, 5188 (1976).
- ³⁵K. Eichhorn, A. Kirfel, J. Grochowski, and P. Serda, *Acta Crystallogr. B* **47**, 843–848 (1991).
- ³⁶F. Oba, M. Choi, A. Togo, and I. Tanaka, *Sci. Technol. Adv. Mater.* **12**, 034302 (2011).
- ³⁷S. Lany and A. Zunger, *Modell. Simul. Mater. Sci. Eng.* **17**, 084002 (2009).
- ³⁸H.-P. Komsa, T. T. Rantala, and A. Pasquarello, *Phys. Rev. B* **86**, 045112 (2012).
- ³⁹P. Blaha, K. Schwarz, G. Madsen, D. Kvasnicka, and J. Luitz, *WIEN2k, An Augmented Plane Wave Local Orbitals Program for Calculating Crystal Properties* (Karlheinz Schwarz, Techn. Universität Wien, Austria, 2001).
- ⁴⁰M. O. Krause and J. H. Oliver, *J. Phys. Chem. Ref. Data* **8**, 329 (1979).
- ⁴¹O. Mishima and K. Era, in *Electric Refractory Materials*, edited by Y. Kumashiro (Marcel Dekker, Inc., New York, 2000), p. 495.